

1-1-2017

Transmission power control using state estimation-based received signal strength prediction for energy efficiency in wireless sensor networks

RAMAKRISHNAN SABITHA

KRISHNA BHUMA

THANGAVELU THYAGARAJAN

Follow this and additional works at: <https://journals.tubitak.gov.tr/elektrik>



Part of the [Computer Engineering Commons](#), [Computer Sciences Commons](#), and the [Electrical and Computer Engineering Commons](#)

Recommended Citation

SABITHA, RAMAKRISHNAN; BHUMA, KRISHNA; and THYAGARAJAN, THANGAVELU (2017) "Transmission power control using state estimation-based received signal strength prediction for energy efficiency in wireless sensor networks," *Turkish Journal of Electrical Engineering and Computer Sciences*: Vol. 25: No. 1, Article 45. <https://doi.org/10.3906/elk-1503-222>

Available at: <https://journals.tubitak.gov.tr/elektrik/vol25/iss1/45>

This Article is brought to you for free and open access by TÜBİTAK Academic Journals. It has been accepted for inclusion in Turkish Journal of Electrical Engineering and Computer Sciences by an authorized editor of TÜBİTAK Academic Journals. For more information, please contact academic.publications@tubitak.gov.tr.

Transmission power control using state estimation-based received signal strength prediction for energy efficiency in wireless sensor networks

Ramakrishnan SABITHA*, Krishna BHUMA, Thangavelu THYAGARAJAN

Department of Instrumentation Engineering, MIT Campus, Anna University, Chennai, Tamil Nadu, India

Received: 25.03.2015

Accepted/Published Online: 31.01.2016

Final Version: 24.01.2017

Abstract: In battery-operated wireless sensor networks, the quality of service requirements such as throughput and energy efficiency must be stringently maintained while the least amount of energy is consumed. Since a major portion of energy is spent by the transceiver operations, transmission power control (TPC) in the medium access control (MAC) layer can bring about considerable energy efficiency. Since TPC algorithms will have a direct impact on the received signal strength index (RSSI) at the receiver, RSSI is the primary input parameter for any TPC algorithm. The objective of the proposed work is to decide on the exact value of transmission power required for the next transmission that will ensure an RSSI just above the threshold level at the receiver. Since this involves estimation of RSSI for the next transmission, we propose three state estimation techniques, namely Kalman filter (KF), extended KF (EKF), and unscented KF (UKF) to predict the RSSI accurately. This predicted value is used as an input for an artificial neural network (ANN)-based TPC algorithm. The effectiveness of the estimation techniques is verified by the prediction error. The accuracy of prediction is reflected in the TPC algorithm in terms of reduced power utilization.

Key words: Wireless sensor networks, RSSI prediction, state estimation techniques, transmission power control, Kalman filter, neural network controller

1. Introduction

In a wireless sensor network (WSN), the nodes are often separated by short distances due to clustering of nodes in a small geographical area. Therefore, energy conservation can be maximized using appropriate transmission power control (TPC) techniques. Received signal strength index (RSSI) is the most important parameter used in TPC algorithms. We can categorize TPC techniques as reactive type and proactive type. In the former type, the RF power required for the next transmission is decided on based on the currently measured RSSI. Since the channel characteristics of a WSN environment are neither deterministic nor static, such decisions may not be reliable, particularly in the case of large transmission intervals and also in the case of highly noisy channel environments. In the latter type, the decision is made based on the predicted RSSI of the next transmission. Clearly, proactive TPC will perform better than reactive TPC in terms of energy conservation. In our paper, we propose a proactive type TPC algorithm involving a Kalman filter (KF) and its variants, namely extended KF (EKF) and unscented KF (UKF), for predicting the RSSI of the next transmission and compare the performance. The predicted RSSI is used in the ANN-based TPC algorithm. Simulation studies are performed for each method for a given duration in a chosen WSN scenario. The average power utilized and the network throughput are recorded for all the proposed algorithms and the performance is analyzed. We

*Correspondence: sabitha.ramakrishnan@gmail.com

also compare the performance of the proposed algorithms with the fuzzy logic-based TPC and Markov-based TPC proposed earlier by the authors. It is observed that UKF-based RSSI predictions are very accurate and hence the TPC algorithm using UKF predictions offers the best saving in energy without compromising the throughput.

2. Related work

The literature on KFs shows that they can be applied for resolving a variety of issues in WSNs. In a typical data-driven WSN environment, a selected number of nodes can be identified from the available numerous sensors, to relay the sensor data, so that redundancy can be avoided. To achieve this, a multistep sensor selection strategy using a KF has been proposed [1] to schedule sensors that would transmit for the next T number of steps. When compared to the standard KF, the particle filter gives highly accurate estimates but at a very high computational cost. In order to reduce the cost, the quantized KF algorithm [2] can be used by deciding on the number of bits required to maintain the mean squared error within a given tolerance. By combining signal to noise ratio (SNR) and the link quality index (LQI), a KF-based effective SNR prediction [3] can be done in order to improve the accuracy of prediction in channel link capacity. A distributed KF (DKF) has been proposed [4] for solving the problems of out-of-sequence measurements and clusterized topologies in WSN. The authors of this paper use a DKF for filtering the asynchronous arrival of information and for deciding on the optimal amount of node information to be stored in the cluster heads in mobile WSNs. TPC has been used in CDMA networks [5] for overcoming near-far problems and noise interference. It has also been used in GSM networks [6] where the power control is done at the mobile end with the guidance of the base station. In the WSN literature, topology control algorithms [7] along with TPC are used where the primary objective is to maintain network connectivity. TPC can also be used for enhancing the link quality blacklisting of nodes in a WSN [8]. An on-demand TPC (ODTPC) [9] uses the fading channel model and the RSSI to arrive at an approximate transmission power that will ensure successful communication in a WSN. A factor M is used to set a margin for the transmission power and it is adjusted dynamically. The authors claim that this method is simple and hence reduces the initialization overhead. A further improvement to ODTPC is the adaptive ODTPC [10], which uses a KF to predict the future RSSI values by incorporating the time-varying fading channel conditions. These values are then used to regulate the transmission power level with the help of ODTPC strategy. In our paper, KF-based algorithms are used for predicting the RSSI while TPC is implemented using an ANN controller. An ANN gives better performance than fuzzy logic control (FLC) as it has inherent weight adjustments for improving the accuracy. The literature shows that FLC has been utilized extensively for several energy efficient techniques in wireless sensor networks. The RSSI together with the link quality index (LQI) of the channel can be utilized for TPC [11] to improve network efficiency. Fuzzy logic-based cluster head selection has been proposed as an enhancement for the low energy adaptive clustering hierarchy (LEACH) protocol [12], which uses the remaining node energy and distance of separation between nodes as the two inputs to the FLC block. A dynamic TPC algorithm has been proposed that utilizes the LQI and RSSI values pertaining to all the neighbor nodes for adjusting the transmission power [13]. RSSI predictions have been utilized for localization of the nodes in a WSN [14]. However, the RSSI values will drastically vary between outdoor and indoor deployments. Moreover, due to time varying characteristics of the channel and random noise disturbances affecting the channel, RSSI values will undergo fluctuations that may lead to inaccuracies in RSSI-based localization. Unlike localization, an RSSI-based TPC algorithm can be designed with very good accuracy. Jiang et al. [15] propose a KF-based local mean power estimation for the nodes in a cellular mobile network by modeling the channel's shadowing as

a first order auto regressive process and show that the KF-based estimate of local mean power is more accurate than the conventional window-based estimation techniques. However, as explained by the authors, the KF method works well only for the slowly varying shadow component in the channel. For fast fading channels, the KF will induce a linearization error. If the EKF method is used, the linearization process of the EKF will reduce the linearization error. However, due to the omission of higher order terms in the EKF approximation, large errors may occur in the posterior mean and covariance of the updates, resulting in suboptimal performance. If the UKF method is used, the error is drastically reduced as it captures the true mean and covariance of the state variable to the second order Taylor's series expansion. In our paper, we discuss all these three methods and compare their performance with respect to the RSSI prediction accuracy. We also show that the prediction accuracy is effectively reflected in the energy conserved by the TPC algorithm that utilizes the RSSI predictions. The rest of the paper is organized as follows. In the next section, the state estimation techniques used for RSSI prediction are discussed. The ANN-based TPC algorithm is presented in Section 4. In Section 5, we analyze the performance of the TPC algorithms while using the various RSSI prediction techniques discussed. Finally, we present the conclusion in Section 6.

3. RSSI prediction using state estimation techniques

The first step in the design of any TPC algorithm is to set up the WSN environment. We choose a star topology WSN scenario with specifications as given in Table 1.

Table 1. Specifications of the chosen WSN environment.

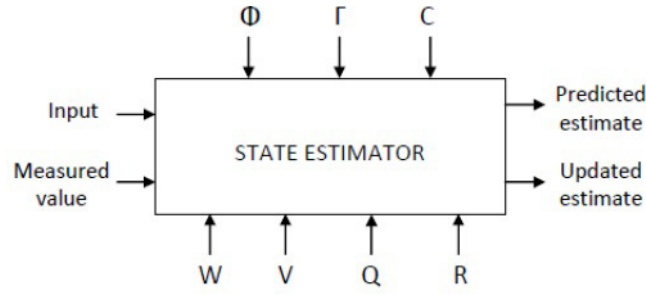
Parameter	Chosen values
No. of nodes	16
Mobility of nodes	Random way point (<1 m/s)
Data rate	250 kbps
Packet size/interpacket delay	64 bytes/1 s
Transmission power range	0.1 mW to 1 mW
Threshold RSSI	-85 dBm
Wireless channel	Fading channel with log-normal shadowing
Channel noise levels:	Low noise channel (60 dB SNR/sample) Medium noise channel (40 dB SNR/sample) High noise channel (20 dB SNR/sample)

The next step is to design the RSSI estimation algorithm. Figure 1 shows the general block diagram of a state estimator and the predictor-corrector loop for RSSI estimation.

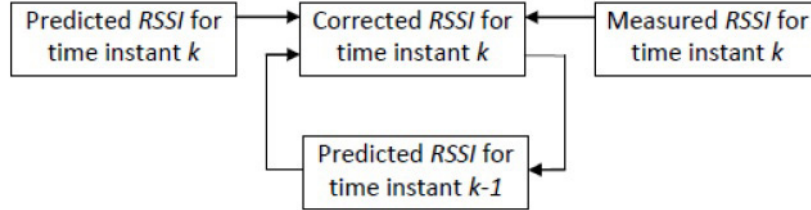
Here N is the number of states, Φ is the $N \times N$ state matrix, Γ is the $N \times 1$ input matrix, C is the $1 \times N$ output matrix, W is the process noise, V is the measurement noise, Q is the process covariance matrix, and R is the measurement covariance matrix.

3.1. KF-based RSSI estimation

The KF is a scalar filter that can offer a minimum mean square error prediction of the RSSI in a noisy environment using linear time-update and measurement-update equations. The KF method offers a better estimation of local mean power when compared to the window-based estimators such as sample average estimator, uniformly minimum variance unbiased estimator, and the maximum likelihood estimator [15]. The KF method proposed in our paper differs from that proposed by Jiang et al. in three major aspects. Firstly, we utilize the fading channel model with log-normal shadowing and propose the KF method to predict the



(a) Overall Block diagram



b) Predictor-corrector loop of the state estimator for RSSI prediction

Figure 1. Block diagram of the state estimator used for RSSI prediction.

RSSI, whereas Jiang et al. utilize the AR(1) model for the shadowing process and propose the KF method to predict the shadowing. Secondly, in our KF equations, we include the transmission power as an input in our KF equations, whereas Jiang et al. do not include it in theirs. The reason for this is justified based on necessity. Jiang et al. propose their KF-based power estimation method for a cellular mobile network in which the base stations do not control their transmission power. The RSSI variations at the mobile node are only due to the channel fading characteristics and node mobility and not due to variations in transmission power at the base station. In our paper, we utilize the KF-based RSSI predictions for TPC in a WSN where all the EDs control their transmission power dynamically. Such an adaptive transmission power causes sudden large variations in the RSSI. Hence, the transmission power is used as an input variable in our KF equations, thus taking into account the effect of TPC on RSSI variations. Finally, Jiang et al. propose the KF method only, whereas we propose KF, EKF, and UKF methods for RSSI prediction and compare their performance with respect to RSSI prediction accuracy. We use the predicted RSSI values from each of these methods in our TPC algorithms and compare the performance with respect to the average power utilized and network throughput.

The fading channel with log-normal shadowing [16] considered for our WSN environment is given in Eq. (1).

$$10 \log(P_r) = 10 \log \left[P_t G_t G_r \left(\frac{\lambda}{4\pi} \right)^2 \left(\frac{d_o}{d} \right)^3 \right] + X_\sigma, \quad (1)$$

where P_r is the received power, $10 \log(P_r)$ the RSSI, P_t the transmission power, λ the wavelength of signal, d the separation between the end device (ED) and the coordinator (COORD), G_t and G_r the gain of transmitting and receiving antennas, and X_σ the additive white Gaussian noise (AWGN) with zero-mean and standard deviation σ . d_o is the reference distance at which maximum RSSI is received. Starting from d_o , the RSSI decays with increase in distance d as per Eq. (1). For simplicity, the value of d_o is considered 1 m. The time update equation of KF projects the current state ahead in time. The measurement update equation of KF adjusts the projected estimate by an actual measurement at that time. Initially, the mathematical state space model required to implement the KF algorithm is obtained through simulation with the transmission power as the input, the fading channel with log-normal shadowing characteristics governed by Eq. (1) as the process and the RSSI as the output. The discrete linear state space model obtained for the KF [17] is given by Eqs. (2)

and (3).

$$X(k) = \Phi \times X(k - 1) + \Gamma \times U(k - 1) + W(k), \quad (2)$$

$$Y(k) = C \times X(k) + V(k), \quad (3)$$

$$\Phi = \begin{bmatrix} 1.0010 & -0.00403 & -0.00097 & 0.00337 \\ -0.0007 & 0.95219 & -0.07159 & -0.20753 \\ -0.0085 & -0.08797 & 0.15480 & -0.00155 \\ 0.0441 & 0.11537 & -0.4596 & 0 & 0.05864 \end{bmatrix}, \quad (4)$$

$$\Gamma = \begin{bmatrix} 2.9643e - 014 \\ 3.6279e - 017 \\ -1.0468e - 015 \\ 0 \end{bmatrix}, \quad (5)$$

$$C = [289.4 - 0.2119 - 0.26992 - 0.43961], \quad (6)$$

where $X(k)$ is the state vector given by $X(k) = [X(1)X(2)X(3)X(4)]$, $U(k) = Ptsrc$, the transmission power; $Y(k) = \text{RSSI}$; $W(k) = \text{process noise} \sim N(0, Q)$, where $Q = \text{process noise covariance}$. $V(k) = \text{measurement noise} \sim N(0, R)$, where $R = \text{measurement noise covariance}$. $W(k)$ and $V(k)$ are AWGN. Thus, the input matrix Γ , the state matrix Φ , and the output matrix C for the chosen WSN are determined using parameter estimation, one of the techniques for system identification as given above. For the above model, the KF algorithm can be implemented to predict the RSSI of the next transmission, i.e. $Y(k + 1)$. From Eqs. (2) and (3), the time update equations of the KF algorithm can be formulated as given in Eqs. (7) and (8). The measurement update equations are formulated as given in Eqs. (9), (10), and (11).

$$X^\wedge(k|k - 1) = \Phi \times X^\wedge(k - 1|k - 1) + \Gamma \times U(k - 1), \quad (7)$$

$$P(k|k - 1) = \Phi \times P(k - 1|k - 1) \times \Phi^T + Q, \quad (8)$$

$$\text{Kalman gain } (K_k) = P(k|k - 1) \times C^T \times C \times P(k|k - 1) \times C^T + R^{-1}, \quad (9)$$

$$X^\wedge(k|k) = X^\wedge(k|k - 1) + K_k \times Y(k) - C \times X^\wedge(k|k - 1), \quad (10)$$

$$P(k|k) = (I - K_k \times C) \times P(k|k - 1). \quad (11)$$

After each time update and measurement update cycle, the process is repeated with the previous estimates to project or predict the new estimates.

3.2. Extended KF-based RSSI prediction

The KF addresses the estimation of a state vector using a linear model of a dynamic system. Hence the KF causes a linearization error, which can be overcome by applying a linearization procedure. The resulting filter is called an EKF. The state space model equations of a nonlinear dynamic system [17] are given by Eqs. (12) and (13).

$$X(k) = f(X(k - 1), U(k - 1)) + W(k), \quad (12)$$

$$Y(k) = H(X(k), k) + V(k), \quad (13)$$

where $f(X(k-1), k)$ and $H(X(k), k)$ denote a nonlinear transition matrix and measurement matrix, respectively, that may be time-variant. To linearize the state space model, for every time instant, the most recent state estimate is taken, which is either $X(k|k-1)$ or $X(k|k)$ depending on the particular function being considered. Once a linear model is obtained, the standard KF equations can be applied. The approximation proceeds in two stages. In the first stage, the following two matrices are constructed:

$$\Phi(k) = \left. \frac{\partial f [x(k-1), k]}{\partial X} \right|_{X=\hat{X}(k-1|k-1)}, \quad (14)$$

$$C(k) = \left. \frac{\partial H [x(k), k]}{\partial X} \right|_{X=\hat{X}(k|k-1)}. \quad (15)$$

In stage 2, we apply first-order Taylor series approximation of the nonlinear functions $f(X(k-1), k)$ and $H(X(k), k)$ to estimate $X^\wedge(k-1|k-1)$ and $X^\wedge(k|k-1)$, respectively. Eqs. (12) and (13) are thus approximated as follows:

$$X(k) \approx \Phi(k-1) \times X(k-1) + f(X^\wedge(k-1|k-1), U(k-1)) - \Phi(k-1) \times X^\wedge(k-1|k-1) + W(k), \quad (16)$$

$$Y(k) \approx C(k) \times X(k) + H(X^\wedge(k|k-1)) - C(k) \times X^\wedge(k|k-1) + V(K), \quad (17)$$

It can be seen that Eqs. (16) and (17) are of the same form as that of Eqs. (2) and (3) and hence the KF algorithm can be applied consequently. Here the Taylor's series approximation has to be applied only for the measurement equation as it is nonlinear in nature and varies exponentially with distance. Φ and Γ matrices are unaltered. Thus, the C matrix before and after the first-order Taylor's approximation is shown in Eq. (18) and Eq. (19) respectively.

$$C = [-289.4 \times \exp(-X1)0.2119 \times \exp(-X2)0.26992 \times \exp(-X3) - 0.043961 \times \exp(-X4)], \quad (18)$$

$$C = [289.4 \times \exp(-X1) - 0.2119 \times \exp(-X2) - 0.26992 \times \exp(-X3)0.043961 \times \exp(-X4)], \quad (19)$$

The time update and measurement update equations of the EKF algorithm are given as follows:

$$X^\wedge(k|k-1) = f(X^\wedge(k-1|k-1), U(k-1)), \quad (20)$$

$$P(k|k-1) = \Phi(k) \times P(k-1|k-1) \times \Phi(k)^T + Q, \quad (21)$$

$$\text{Kalman gain } (K_k) = P(k|k-1) \times C(k)^T \times [C(k) \times P(k|k-1) \times C(k)^T + R]^{-1}, \quad (22)$$

$$X^\wedge(k|k) = X^\wedge(k|k-1) + K_k \times Y(k) - C(k) \times X^\wedge(k|k-1), \quad (23)$$

$$P(k|k) = (I - K_k \times C(k)) \times P(k|k-1). \quad (24)$$

It is to be noted that the function $C(k)$ in the EKF helps to propagate only the relevant component of the measurement information, thus providing an accurate estimate.

3.3. UKF-based RSSI prediction

In the EKF, the state distribution is approximated, which is then propagated analytically through the first-order linearization of the nonlinear system. As the higher order terms are neglected, these approximations may introduce large errors in the posterior mean and covariance of the updated random state variable, resulting in suboptimal performance and sometimes divergence of the filter. The UKF addresses this approximation issue of the EKF. The state distribution is represented by a random state variable, but specified using a set of sample points. These sample points completely capture the true mean and covariance of the random state variable, and when propagated through the true nonlinear system, capture the posterior mean and covariance accurately to the second-order Taylor series expansion for any nonlinearity. The state space model of the WSN is given by Eqs. (4), (5), and (18), similar to that used for the EKF algorithm. For the state vector of length N , $2N + 1$ uniformly spaced sample points are chosen as follows:

$$X^{\wedge i}(k-1|k-1) = X^{\wedge}(k-1|k-1) \text{ For } L = 0, \tag{25}$$

$$X^{\wedge i}(k-1|k-1) = X^{\wedge}(k-1|k-1) + \sqrt{(N + \text{kappa}) \times P[(k-1)|(k-1)]} \text{ For } L = 1 \text{ to } N, \tag{26}$$

$$X^{\wedge i}(k-1|k-1) = X^{\wedge}(k-1|k-1) - \sqrt{(N + \text{kappa}) \times P[(k-1)|(k-1)]} \text{ For } L = N + 1 \text{ to } 2N. \tag{27}$$

The weights associated with each of the sample points are calculated as follows:

$$W^i = \frac{\text{kappa}}{N + \text{kappa}} \text{ For } L = 0, \tag{28}$$

$$W^i = \frac{1}{2 \times (N + \text{kappa})} \text{ For } L \neq 0, \tag{29}$$

In Eqs. (26) to (29), $Kappa$ is the tuning factor [17] and usually taken to be $3 - N$ for log-normally distributed random variables. The sample points obtained from Eqs. (25) to (27) are propagated through the nonlinear dynamic system process equation to get the sample predicted mean. From the sample predicted mean, the predicted mean and predicted covariance are calculated as follows:

$$X^{\wedge}(k|k-1) = \sum W^i \times X^{\wedge i}(k|k-1) \text{ For } i = 0, 1, 2, \dots, 2N, \tag{30}$$

$$P(k|k-1) = \sum W^i \times \{ [X^{\wedge i}(k|k-1) - X^{\wedge}(k|k-1)] \times [X^{\wedge i}(k|k-1) - X^{\wedge}(k|k-1)]^T \text{ For } i = 0, 1, \dots, 2N. \tag{31}$$

Similarly the sample points of the predicted mean are calculated and passed through the measurement equation of the nonlinear dynamic system to get the sample output as follows:

$$X^{\wedge i}(k|k-1) = X^{\wedge}(k|k-1) \text{ For } L = 0, \tag{32}$$

$$X^{\wedge i}(k|k-1) = X^{\wedge}(k|k-1) + \sqrt{(N + \text{kappa}) \times P(k|k-1)} \text{ For } L = 1, 2, \dots, N, \tag{33}$$

$$X^{\wedge i}(k|k-1) = X^{\wedge}(k|k-1) - \sqrt{(N + \text{kappa}) \times P(k|k-1)} \text{ For } L = N + 1, N + 2, \dots, 2N. \tag{34}$$

The sample predicted output is obtained using Eq. (35) and the predicted output is then obtained using Eq. (36). The innovation covariance matrix $P\gamma\gamma$ describes the effects of time on the covariance matrices of output estimation errors. It is determined as shown in Eq. (37). Cross covariance matrix $Px\gamma$, determined by Eq. (38), describes the effects of time on the covariance matrices of state estimation error and output estimation error.

$$Y^{\wedge i}(k|k-1) = H[X^{\wedge i}(k|k-1)], \tag{35}$$

$$Y^{\wedge}(k|k-1) = \sum W^i \times Y^i(k|k-1) \text{ For } i = 0, 1, 2, \dots, 2N, \tag{36}$$

$$P\gamma\gamma = \sum W^i \times [Y^i(k|k-1) - Y(k|k-1)] \times [Y^i(k|k-1) - Y(k|k-1)]^T, \tag{37}$$

$$Px\gamma = \sum W^i \times [X^i(k|k-1) - X(k|k-1)] \times [Y^i(k|k-1) - Y(k|k-1)]^T. \tag{38}$$

Next the UKF measurement updates are obtained as follows:

$$K_k = Px\gamma * P\gamma\gamma^-, \tag{39}$$

$$X^{\wedge}(k|k) = X^{\wedge}(k|k-1) + K_k \times [Y(k) - Y^{\wedge}(k|k-1)], \tag{40}$$

$$P(k|k) = P(k|k-1) - K_k \times P\gamma\gamma \times, \tag{41}$$

where $P(k|k)$ is the corrected co-variance estimate and K_k is the Kalman gain. The plots of predicted RSSI vs. actual RSSI for the three proposed state estimation techniques, namely KF, EKF, and UKF, are shown in Figure 2 for low noise channel.

From the above plots, it may be observed that the KF gives high error in the short distance (high RSSI) range whereas the EKF gives high error in the long distance (low RSSI) range. The UKF gives the best prediction over the range of RSSI values from -40 dBm to -90 dBm. This is attributed to its high accuracy of prediction superior to the other two methods. The standard error of the predicted RSSI is calculated as

$$\varepsilon_p(y) = \sqrt{\frac{1}{(n-2)} \left[\sum (y-\bar{y})^2 - \frac{[\sum (x-\bar{x})(y-\bar{y})]^2}{\sum (x-\bar{x})^2} \right]}, \tag{42}$$

where x and y are the individual samples, \bar{x} and \bar{y} are the sample means average of the actual and predicted RSSI, respectively, and n is the number of samples. Accordingly the standard error is given in Table 2 for the three estimation methods in the three different noisy channels.

Table 2. Standard error of RSSI prediction in the three different noisy channels.

RSSI estimation method	Error in low noise channel (dBm)	Error in med. noise channel (dBm)	Error in high noise channel (dBm)
UKF	1.0177	1.2626	7.2006
EKF	0.5334	1.4389	8.8320
KF	1.1852	3.5172	9.0808

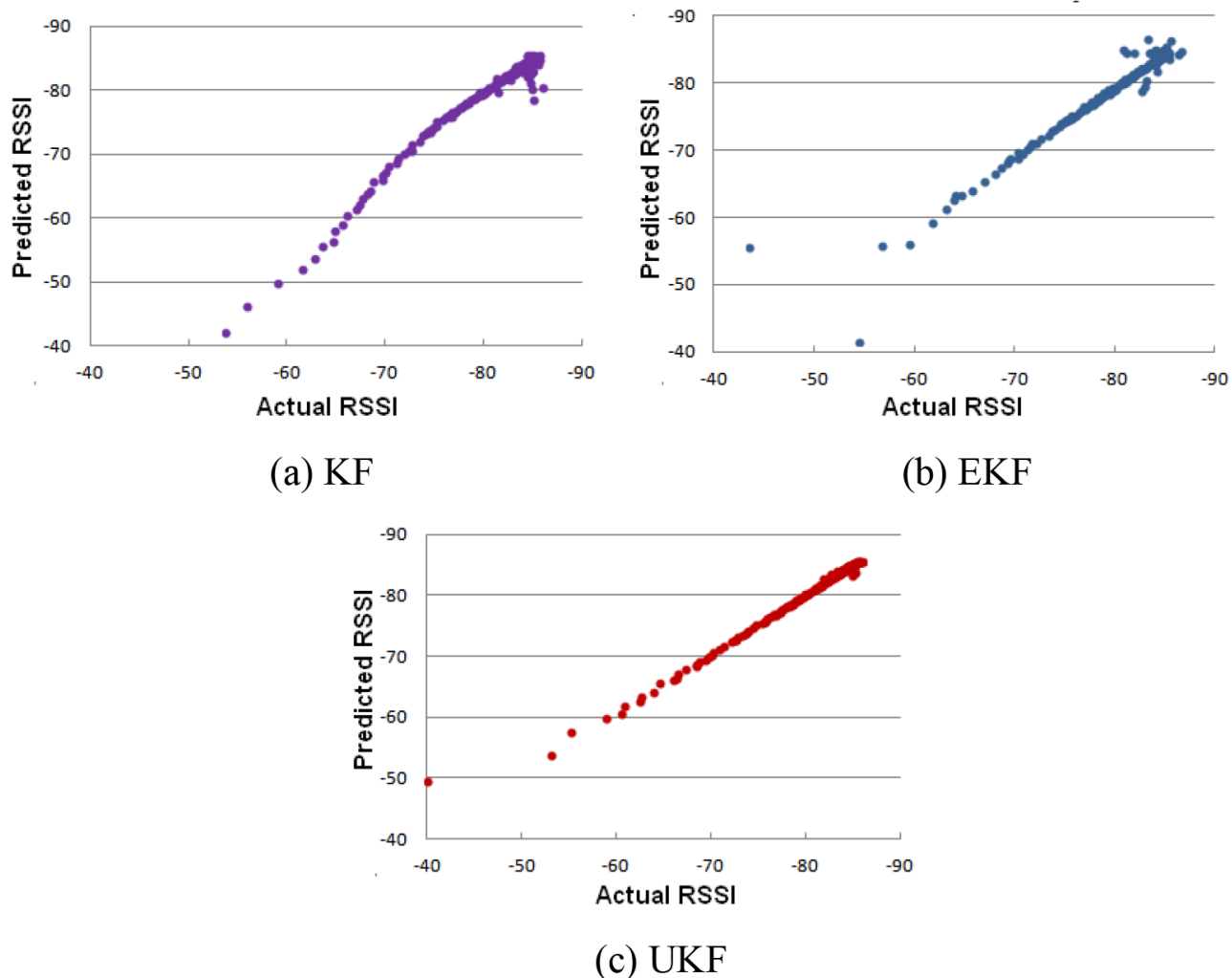


Figure 2. Predicted vs. actual RSSI in a low noise channel while using the three state estimation techniques.

It is clear that the UKF gives the best prediction with minimum error under all channel noise conditions. The next section presents the ANN-based TPC algorithm that utilizes this predicted RSSI value for deciding on the required transmission power (P_{treq}).

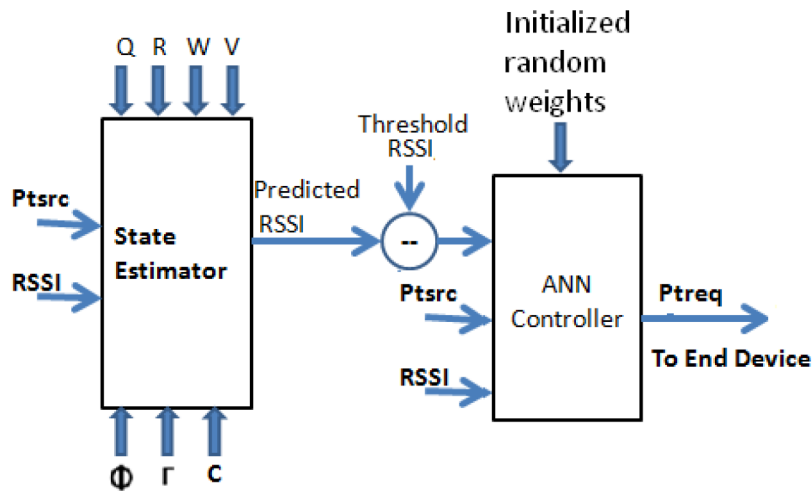
4. ANN-based TPC algorithm

The predicted value of RSSI obtained from the state estimation block is given as one of the inputs to an ANN-based transmission power control algorithm (ANN-TPC) implemented in the coordinator node (COORD), which is a full function device (FFD). The end device (ED), which is usually a reduced function device (RFD), does not implement computationally intense TPC algorithms in order to conserve the available energy. The COORD receives the packet sent by the ED with an RSSI that is measurable by its RF circuit. The value of the transmission power P_{tsrc} used by ED is sent by the ED as part of the MAC payload, which is extracted by the COORD on reception. Based on these two sets of data, the state estimator predicts the RSSI for the next transmission. A feed forward ANN is used for deciding on P_{treq} . The design parameters of the ANN are shown in Table 3.

Table 3. ANN design parameters.

Parameter	Values
No. of input layers Neurons	3
No. of hidden layers Neurons	1
No. of output layers neurons	1
Learning algorithm	Back propagation algorithm

The inputs to the ANN block are the estimated RSSI (for the next transmission), the actual RSSI (of the currently received signal), and P_{tsrc} (used by the transmitter for the currently received signal). The threshold value of RSSI is fixed as -85 dBm. The typical receiver sensitivity of a transceiver is -94 dBm (for CC2420 RF transceiver). However, the noise floor is kept at a higher level because the signal to interference noise ratio (SINR) may increase [18] depending on the terrain of deployment and also on the interference from co-existing networks such as IEEE 802.11 wireless local area network (WLAN). A block diagram of the ANN used for TPC is shown in Figure 3.

**Figure 3.** ANN block diagram used for TPC.

The three different TPC techniques are named KF-TPC, EKF-TPC, and UKF-TPC, based on the method used for RSSI estimation. The ANN controller part is common to all three techniques. The simulation results obtained for low noise channel are shown in Figure 4. Under two extreme conditions, TPC is not possible: (i) when the RSSI is below the threshold for maximum P_{tsrc} , there is no further possibility of increasing the transmission power and (ii) when the RSSI is high for minimum P_{tsrc} , there is no possibility of decreasing the P_{tsrc} any further. In all other conditions, the TPC algorithm is executed. It is observed that all the TPC algorithms save considerable power when compared to the conventional MAC standard IEEE 802.15.4.

It is observed that P_{treq} increases in a gradual fashion from -10 dBm to 0 dBm for the distance varying from 1 m to 150 m. The intermittent glitches in P_{treq} seen in Figure 4 are due to the controlling action by the ANN controller. When the noise level in the channel increases, the estimation error increases as shown earlier in Table 2. Hence the controller action is affected and the throughput degrades due to occasional packet drops.

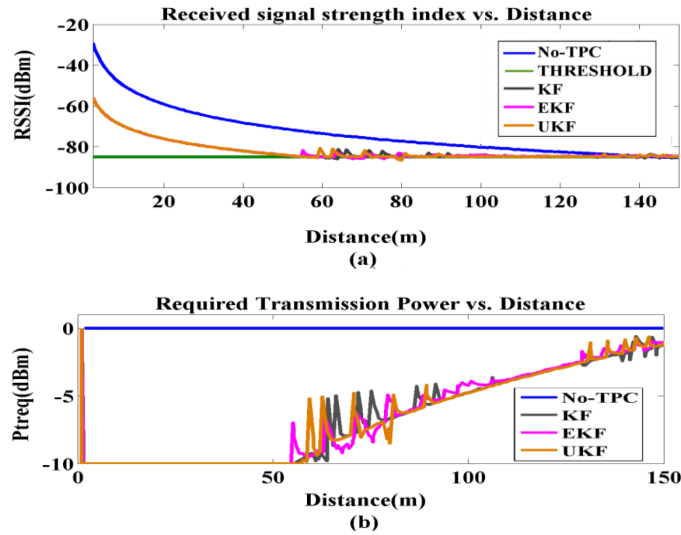


Figure 4. (a) RSSI vs. distance and (b) Preq vs. distance in a low noise channel.

5. Results and discussion

Two important performance parameters are considered for analysis, namely throughput and the average power utilized. Throughput of a WSN is the percentage of packets successfully delivered to the receiver as given in Eq. (43).

$$\text{Throughput}(\%) = \frac{\text{Packets_delivered}}{\text{Packets_transmitted}} \times 100, \tag{43}$$

Average power utilized is determined using Eq. (44).

$$P_{avg} = \frac{1}{N} \sum_{i=1}^N P_i, \tag{44}$$

where P_{avg} is the average transmission power, N is the total number of transmissions, and P_i is the transmission power of individual transmissions. We compare the performance of the proposed TPC algorithms along with two other TPC algorithms proposed earlier, namely, fuzzy logic-based TPC (FTPC) [19] and Markov-based TPC (MTPC) [20]. We test the performance of the TPC algorithms on the same WSN scenario as given in Table 1 earlier and compare the results. The FTPC and MTPC algorithms are described briefly in the next section.

5.1. Fuzzy logic-based TPC using RSSI and source transmission power

In FTPC, a fuzzy logic control (FLC) block is designed with two inputs, namely the transmission power used at the source node (P_{src}) and the corresponding signal strength at the receiver node ($RSSI$) and one output, namely the required transmission power (P_{req}). The FTPC algorithm offers all the advantages of FLC such as simplicity and scalability. The rule base matrix of FTPC is formulated using the knowledge base acquired through simulation and real time testing. The two drawbacks of the FTPC algorithm are as follows. Firstly, the rule-base matrix plays a vital role in deciding the performance of the TPC algorithm. Secondly, the decision of P_{req} for the next transmission is based on the current values of P_{src} and $RSSI$. The algorithm does not involve RSSI estimation and hence it is likely that the decision of P_{req} may not be accurate, particularly, in

a high noise channel, resulting in either a high value of P_{treq} , which may result in wastage of energy, or a low value of P_{treq} below the required level, which may cause packet drops.

5.2. Markov-based RSSI prediction and fuzzy logic-based TPC

In MTPC, the communication in the WSN is defined as a Markov model and a Markov chain is used for predicting the next RSSI value. The predicted RSSI is given as input to the FLC block for deciding on P_{treq} . The design parameters for the FLC block of MTPC are the same as that for FTPC as explained in Section 5.1 except that the input variables are $RSSI$ and change in RSSI (δr). The Markov-based RSSI prediction is sufficiently accurate when the noise characteristics are wide-sense stationary. This ensures that no relevant channel history needs be considered while deciding P_{treq} . From the data set collected during test runs, the WSN is modeled as a Markov chain with the state space representing the change in RSSI (δr). A transition probability matrix, formulated from the collected data, has entries representing the probabilities for the next expected change in RSSI value based on the current change. For any given current state, there is a state vector that is a particular row in the matrix that gives the probability values for the next state. The WSN environment is modeled as an ergodic Markov process, meaning that the WSN is an irreducible as well as aperiodic system. The constraint in MTPC is the formation of an exhaustive initial data set to create the transition probability matrix, which is the basis for estimating the next RSSI value.

5.3. Comparison of the performance of the TPC algorithms

In the TPC algorithms proposed in this paper, we predict the RSSI of the next transmission accurately to maintain the transmission power at an optimal level. This conserves the energy considerably, the best among them being UKF-TPC. Throughput for all the proposed TPC techniques was found to be comparable in low and medium noise channels. In high noise channel, UKF-TPC was observed to give a better throughput than all other TPC techniques. The results are tabulated in Table 4.

Table 4. Comparison of the performance of the TPC algorithms.

Channel condition	Throughput (%)					Average power (dBm)				
	KF-TPC	EKF-TPC	UKF-TPC	M-TPC	FTPC	KF-TPC	EKF-TPC	UKF-TPC	M-TPC	FTPC
Low noise	92	97	97	93	94	-6.04	-6.30	-6.69	-5.12	-3.78
Medium noise	86	87	90	79	77	-5.73	-6.12	-6.45	-4.81	-3.27
High noise	63	68	79	60	65	-5.51	-6.00	-6.43	-4.23	-2.98

UKF-TPC offers the highest throughput among all the TPC algorithms irrespective of the channel noise level, as is evident from Figure 5. The superior performance of UKF-TPC is attributed to the accurate prediction of RSSI and accurate control of transmission power by the neural network based controller. KF-based algorithms can perform well for linear systems but will fail to predict accurately for nonlinear systems. EKF-based algorithms are suitable for nonlinear systems; however, they are not capable of performing well for multimodal systems. A typical RSSI-vs.-distance curve of a log-normal shadowing model in a channel of varying noise characteristics is always multimodal. Hence, the linearity error in the KF and the multimodal problem in the EKF cause some degradation in performance. MTPC is not on par with the other estimation-based TPC algorithms, because of its memoryless RSSI prediction. The effectiveness of MTPC can improve only if the transition probability matrix suits the channel characteristics for longer durations. However, its overall performance is better than that of FTPC as it uses predicted RSSI for TPC rather than the current RSSI. It

may be observed that FTPC performs slightly better than MTPC under certain conditions but at the expense of high transmission power, which is obvious from Figure 5. Considering both throughput and average power utilized, we observe that the performance of UKF-TPC is far superior to that of the other TPC algorithms discussed in this paper. As explained in Section 3, UKF-TPC captures the posterior mean and covariance of the RSSI accurately to the second-order Taylor series expansion for any nonlinearity and hence offers better prediction of RSSI than all other prediction algorithms. Hence, UKF-TPC offers the best energy conservation when compared with MTPC, FTPC, KF-TPC, and EKF-TPC.

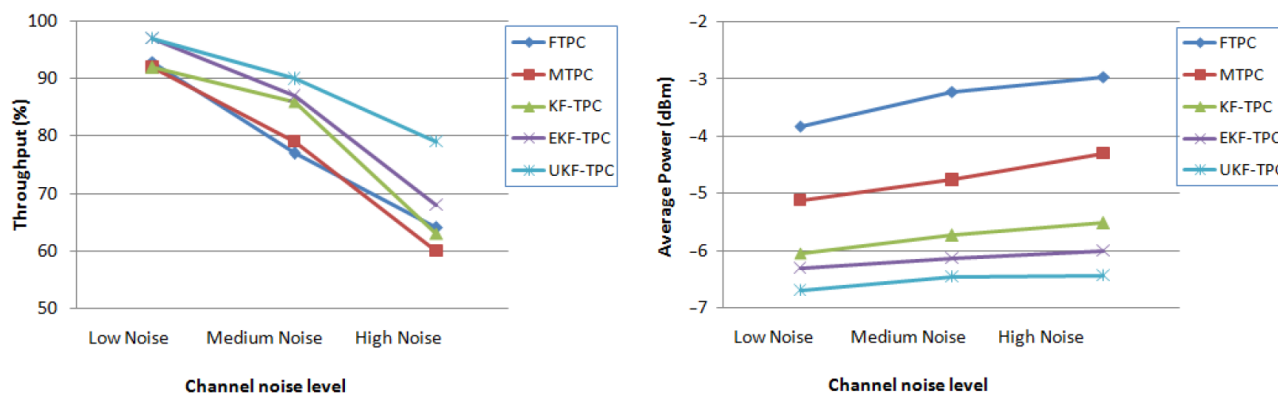


Figure 5. Throughput and average power utilized for the proposed TPC algorithms as compared to two other TPC algorithms.

6. Conclusion

All the three TPC algorithms proposed in this paper and the two algorithms taken for comparison offer a marked saving in the average power without much degradation in the throughput. Among them, UKF-TPC uses the minimum transmission power and offers the maximum throughput, even in high noise channel condition. The computational complexity of UKF-TPC does not affect the performance since the algorithm runs in the coordinator with high processing capability. KF-TPC suffers from errors due to linearization error and EKF-TPC is also not on par with UKF-TPC as it cannot cope with multimodal systems. MTPC is not on par with the other estimation-based TPC algorithms, because of its memoryless RSSI prediction. FTPC performs slightly better than MTPC under specific channel conditions, but at the expense of high transmission power. The superior performance of UKF-TPC is attributed to the accurate prediction of RSSI along with the accurate control of transmission power by the ANN controller.

References

- [1] Mo Y, Ambrosino R, Sinopoli B. Sensor selection strategies for state estimation in energy constrained wireless sensor networks. *Automatica* 2011; 47: 1330-1338.
- [2] Ribeiro A, Schizas JD, Roulmeliotis SI, Giannakis GB. Kalman filtering in WSN. *IEEE Contr Syst Mag* 2010; 30: 66-86.
- [3] Qin F, Dai X, Mitchell JE. Effective SNR estimation for wireless sensor network using Kalman filter. *Ad Hoc Netw* 2013; 11: 944-958.
- [4] Wang C, Chen X, Li W. Energy efficient distributed Kalman filter for wireless sensor networks. In: *IEEE 2014 11th International Conference on Networking, Sensing and Control*; 7-9 April 2014; Miami, Florida: IEEE. pp. 161-166.

- [5] Niida S, Suzuki T, Takeuchi Y. Experimental results of outer loop transmission power control using wideband CDMA for IMT-2000. In: IEEE 2000 51st Vehicular Technology Conference; 15–18 May 2000; Tokyo, Japan: IEEE. pp. 775-779.
- [6] Dutta A, Sarin S. Performance optimization in GSM networks through dynamic power control. In: IEEE 2002 5th International Conference on High Speed Networks and Multimedia Communications Conference; 3–5 July 2002; Jeju Island, Korea: IEEE. pp. 197-201.
- [7] Kubisch M, Karl H, Wolisz A, Zhong LC, Rabaey J. Distributed algorithms for transmission power control in wireless sensor networks. In: IEEE 2003 Wireless Communications and Networking Conference; 20–20 March 2003; New Orleans, USA: IEEE. pp. 558-563.
- [8] Son D, Krishnamachari B, Heidemann J. Experimental study of the effects of transmission power control and blacklisting in wireless sensor networks. In: First Annual IEEE Communications Society Conference on Sensor and Ad Hoc Communications and Networks; 4–7 October 2004; Santa Clara, USA: IEEE. pp. 289-298.
- [9] Kim J, Chang S, Kwon Y. ODTPC On-demand transmission power control for wireless sensor networks. In: International Conference on Information Networking; 23–25 January 2008; Busan, South Korea: IEEE. pp. 1-5.
- [10] Masood MMY, Ahmed G, Khan NM (2012). A Kalman filter based adaptive on demand transmission power control (AODTPC) algorithm for wireless sensor networks. In: International Conference on Emerging Technologies; 8–9 October 2012; Islamabad, Pakistan: IEEE. pp. 1-6.
- [11] Jin S, Fu J, Xu L. The transmission power control method for wireless sensor networks based on LQI and RSSI. In: Communications in Computer and Information Science AsiaSim; 27–30 October 2012; Shanghai, China; pp. 37-44.
- [12] Akbulut A, Öztaş O. Control in networked systems with fuzzy logic. Turk J Elec Eng & Comp Sci 2013; 21: 225-233.
- [13] Sheu JP, Hsieh KY, Cheng YK. Distributed transmission power control algorithm for wireless sensor networks. J Inf Sci Eng 2009; 25: 1447-1463.
- [14] Chen J. RSSI based indoor power localization in Wireless Sensor Network. International Journal of Digital Content Technology and its applications 2011; 5: 408-416.
- [15] Jiang T, Sidiropoulos ND, Giannakis GB. Kalman filtering for power estimation in mobile communications. IEEE T Wirel Commun 2003; 2: 151-161.
- [16] Rappaport T. Wireless Communications Principles and Practices. 2nd edition. London, UK 2002: Pearson.
- [17] Simon D. Optimal State Estimation: Kalman, H Infinity and Nonlinear Approaches. 1st edition. Hoboken, NJ, USA 2006: John Wiley and Sons.
- [18] Kim J, Kwon Y. Interference-aware transmission power control for wireless sensor networks. IEICE T Commun 2008; 11: 3434-3441.
- [19] Sabitha R, Thyagarajan T. Fuzzy logic based transmission power control algorithm for energy efficient MAC protocol in wireless sensor networks. International Journal of Communication Networks and Distributed Systems 2012; 9: 247-265.
- [20] Ramakrishnan S, Thangavelu T. Performance enhancement of fuzzy logic based transmission power control in wireless sensor networks using Markov based RSSI prediction. European Journal of Scientific Research 2011; 59: 68-84.